AIAA'87

AIAA-87-0298

Structure and Radiation Properties of Luminous Turbulent Acetylene/Air Diffusion Flames

J. P. Gore and G. M. Faeth, The Univ. of Michigan, Ann Arbor, MI

AIAA 25th Aerospace Sciences Meeting

January 12-15, 1987/Reno, Nevada

STRUCTURE AND RADIATION PROPERTIES OF LUMINOUS TURBULENT ACETYLENE/AIR DIFFUSION FLAMES

J.P. Gore* and G.M. Faeth+
Department of Aerospace Engineering
The University of Michigan
Ann Arbor, MI 48109-2140

Abstract

An experimental and theoretical study of the structure and radiation properties of luminous, round, turbulent acetylene/air diffusion flames is described. Measurements were made of mean and fluctuating velocities, mean concentrations, laser extinction (514 and 632.8 nm), spectral radiation intensities (1000 - 5550 nm), and radiative heat fluxes. The measurements were used to evaluate structure predictions based on the laminar flamelet concept, and radiation predictions based on a narrow-band model both ignoring and considering turbulence/radiation interactions. State relationships needed for the laminar flamelet concept were found from auxiliary measurements in laminar flames. Predictions were encouraging, however, quantitative accuracy was inferior to earlier findings for luminous flames. This is attributed to the large radiative heat loss fractions of acetylene/air flames (approaching 60 percent of the heat release rate); coupled structure and radiation analysis should be considered for improved results. The findings suggest significant turbulence/radiation interactions (increasing spectral intensities 50 - 300 percent from estimates based on mean properties); and that soot volume fractions may approximate universal functions of mixture fraction in turbulent acetylene/air diffusion flames.

Nomenclature

a	acceleration of gravity
d	burner exit diameter
f	mixture fraction
g	square of mixture fraction fluctuations
I_λ	spectral radiation intensity
k	turbulent kinetic energy
m_o	burner mass flow rate
r	radial distance
Re	burner Reynolds number
u	streamwise velocity
x	height above burner
ε	rate of dissipation of turbulence kinetic energy
ν	kinematic viscosity
ρ	density

Subscripts

c	centerline quantity
o	burner exit condition

Superscripts

(-), (~)	time- and Favre-averaged mean quantity
(-)', (~)"	time- and Favre-averaged root-mean-square fluctuating quantity

Introduction

This paper describes an extension of earlier work concerning the structure and radiation properties of turbulent diffusion flames.[1-8] The objective was to determine whether theoretical methods that were successful for luminous ethylene/air diffusion flames,[8] could be extended to more heavily sooting acetylene/air diffusion flames. Acetylene/air diffusion flames were studied since their soot concentrations are almost an order of magnitude higher than ethylene/air diffusion flames, providing a strong test of analysis. Acetylene/air diffusion flames are also interesting since they have received considerable attention by others.[9-12]

The scalar structure of flames must be known in order to estimate their radiation properties. The laminar flamelet concept, proposed by Bilger[13] and Liew et al.[14] has been successful for estimating the scalar properties of nonluminous flames.[3,6,7] This concept is based on the observation that scalar properties in nonluminous laminar diffusion flames are nearly universal functions of mixture fraction (the fraction of mass at a point which originated from the injector), except near points of flame attachment. These functions have come to be called "state relationships."[3] Turbulent flames are then viewed as wrinkled laminar flames having the same properties; thus, predictions of a single conserved scalar, like mixture fraction, provides a complete description of the scalar properties of the flow. When this approach is applicable, routine measurements or analysis of scalar properties in laminar flames essentially replace the complexities of flame chemistry in turbulent flames.

Extension of these ideas to luminous flames has been considered for ethylene/air diffusion flames.[8] The concentrations of major gas species were found to be nearly universal functions of mixture fraction, in spite of the presence of soot, in laminar ethylene/air diffusion flames. Furthermore, soot volume fraction, which is the main property needed to predict continuum radiation from soot, was also roughly correlated as a function of mixture fraction in laminar flames. Subsequent measurements suggested that universality of soot volume fraction as a function of mixture fraction was preserved for turbulent flames, providing a reasonably successful approach for predicting spectral absorption and emission by soot.[8] In view of the added complexities of soot chemistry, this extension of the laminar flamelet concept is potentially quite valuable for finding the scalar structure and radiation properties of luminous flames, motivating the present study of the flamelet hypothesis for more heavily-sooting acetylene/air flames.

A second issue concerning radiation from luminous turbulent flames involves effects of turbulence/radiation interactions, i.e., errors in radiation predictions based on mean scalar properties due to nonlinearities of radiation properties. This has been studied by comparing predictions based on mean scalar properties with results of a stochastic analysis which seeks to model effects of turbulent fluctuations.[1-8] Findings indicated relatively small effects (ca. 20 percent) of turbulence/radiation interactions for carbon monoxide/air[6] and methane/air[2] diffusion flames. In contrast, hydrogen/air[7] and ethylene/air[8] diffusion flames exhibited very large effects (50-300 percent) of turbulence/radiation interactions. Since fuel type influences turbulence/radiation interactions, the phenomenon was also considered during the present investigation.

*Predoctoral Scholar

+Professor, Associate Fellow AIAA

Earlier studies of turbulent acetylene/air diffusion flames, by Magnussen[11] and Kent and Bastin,[12] provide additional background for the present investigation. Magnussen[11] measured Mie scattering from soot particles, finding that soot was confined to narrow regions associated with turbulent eddies, suggesting that this property is correlated with mixture fraction. Kent and Bastin[12] used laser extinction measurements to study effects of residence time on soot concentrations. They observed that soot concentrations become relatively independent of residence time for sufficiently long residence times, suggesting quasi-equilibrium of soot properties for these conditions. Both observations suggest potential for universality of the state relationship for soot volume fractions, at sufficiently-long residence times, prompting further examination of the effect during the present study.

The paper begins with a brief description of theoretical and experimental methods. Auxiliary measurements in laminar flames, to find state relationships, are then discussed. This is followed by comparison of structure predictions and measurements in the turbulent flames. Laser extinction measurements are then used to study soot volume fraction state relationships in turbulent flames. The paper concludes with consideration of predicted and measured radiant emission properties. The present discussion is brief, more details and a tabulation of data are provided by Gore.[15]

Experimental Methods

Apparatus

The turbulent flame apparatus was identical to past work.[1-8] Acetylene was injected vertically upward from a water-cooled burner within a screened enclosure. The flames were attached at the burner exit using a small coflow of hydrogen.

The laminar flame apparatus was also identical to past work.[6-8] The burner involved vertical injection of acetylene (14.3 mm diameter port) in a concentric coflowing stream of air (102 mm diameter port) within a cylindrical enclosure.

Instrumentation

Instrumentation was generally similar to past work.[1-8] Streamwise mean and fluctuating velocities were measured across the burner exit (x/d = 2) and along the axis of the turbulent flames, using a single-channel laser Doppler anemometer (LDA). Radial velocity fluctuations were also measured at x/d = 2, by rotating the beam plane of the LDA. These measurements were time averages with uncertainties (95 percent confidence) less than 5 percent for mean velocities and less than 10 percent for velocity fluctuations, largely governed by finite sampling times.[15]

Mean concentrations of gaseous species in the laminar and turbulent flames were measured by sampling and analysis with a gas chromatograph. A water-cooled probe, having an inlet diameter of 6.3 mm, was used for isokinetic sampling along the axis of the turbulent flames. A quartz microprobe, having an inlet diameter of 0.1 - 0.2 mm and operating with choked flow at the inlet, was used in the laminar flames. Both probes accumulated deposited-soot and tended to clog in regions having appreciable concentrations of soot; therefore, results for such locations are not reported in the following. Uncertainties in composition measurements (95 percent confidence) are less than 15 percent, largely governed by uncertainties in measuring gas chromatograph peak areas.[15]

Laser extinction measurements were used to study absorption by soot in the turbulent flames. Two wavelengths in the visible (514 and 632.8 nm) were used to determine whether the soot particles satisfied the small-particle Rayleigh-scattering limit, while minimizing effects of radiation emission by soot in the flames. A chopper, operated at 800 Hz, was used to improve signal-to-noise ratios by reducing effects of background and flame radiation. Uncertainties in these measurements (95 percent confidence) are estimated to be less than 10 percent, largely governed by finite sampling times.[15]

Laser extinction measurements at 632.8 nm were used to measure soot volume fractions in the laminar flames, following the deconvolution technique reported by Santoro et al.[16] Soot volume fractions were computed using the refractive-index correlation of Dalzell and Sarofim.[9] Uncertainties in the soot volume fraction measurements (95 percent confidence) are estimated to be less than 20 percent, largely governed by effects of finite sampling times and position accuracy in the build up of errors in the deconvolution procedure.[15]

Spectral radiation intensities were measured with a monochromator, viewing roughly 10 mm diameter (1.2 ° field angle) horizontal paths through the flame axis. Various gratings and order-sorting filters were used for measurements in the 1000 - 5500 nm wavelength range (resolution of 5 percent at 1000 nm and 10 percent at 5500 nm). Uncertainties in intensity levels (95 percent confidence) are estimated to be less than 15 percent, largely governed by the finite sampling times due to the continuous spectral scan.[15]

Radiative heat fluxes were measured at points around the turbulent flames using a gas-purged, water-cooled radiometer (150 ° viewing angle with a sapphire window). Uncertainties (95 percent confidence) in these measurements were less than 10 percent, largely governed by uncertainties in sensor calibrations.[15]

All measurements were repeatable within the uncertainty levels stated above during the course of the study.

Test Conditions

Table 1 is a summary of test conditions for the two turbulent flames that were studied. Initial Reynolds numbers were high enough to provide a reasonably turbulent flow, with residence times varying by roughly a factor of two for the two flames. Initial Richardson numbers were relatively low, however, effects of buoyancy were important near the tip of the flames (defined as the point where the fuel-equivalence ratio, in the mean, was unity along the axis). Initial values of k were estimated from measured streamwise and radial velocity fluctuations, assuming that radial and tangential velocity fluctuations were equal. The resulting values of k_o were relatively high. This is attributed to disturbances from the hydrogen slot within the burner for the relatively low hydrogen flows needed to attach these flows. Initial values of ε were estimated from the rate of decay of k in the potential core of the flow. Radiative heat losses approach 60 percent of the chemical energy release rate in these flames. This is roughly twice the radiative heat loss fractions observed for luminous ethylene/air diffusion flames.[8]

Theoretical Methods

Flame Structure

Analysis of flame structure and radiation properties was identical to past work[1-8] and will only be briefly described. Major assumptions of the structure analysis are as follows: low Mach number boundary-layer flow with no swirl; equal exchange coefficients of all species and heat; buoyancy only affects the mean flow; and negligible radiant energy exchange between various portions of the flame. Except for the last,

Table 1. Summary of Turbulent Flame Test Conditions[a]

Reynolds number[b]	5300	9200
Richardson Number[c] x 10^4	4.5	1.4
u_o(m/s) estimated	10.5	18.1
u_o(m/s) measured	11.8	20.6
$k_o^{1/2}/u_o$	0.13	0.13
Heat Release Rate (kW)	10.5	18.1
Radiative Heat Loss Fraction (%)	57.0	59.0
Fuel Flow Rate (mg/s)	217	376
Hydrogen Flow Rate (mg/s)	1.9	1.9

a Flow directed vertically upward from a 5 mm diameter passage in still air at normal temperature and pressure. Commercial Grade acetylene, Detroit Welding Supply Co.

b $Re = u_o d/\nu$ based on fuel-gas properties at burner exit.

c $Ri = ad/u_o^2$

these assumptions are either justified by test conditions or by acceptable performance for similar diffusion flames.[1-8] The present flames, however, lose an unusually large fraction of their chemical energy release by radiation (ca. 60 percent), which is 2-4 times greater than flames considered during earlier work.[1-8] This behavior suggests significant radiant energy exchange within the flames; thus, the last assumption is questionable. Nevertheless, the assumption is adopted as a first approximation, in order to avoid the complexity and increased computation costs required for coupled structure and radiation analysis. Flow properties were found using a Favre-averaged k-ε-g turbulence model, proposed by Bilger,[17] with specific modifications and empirical constants due to Jeng and Faeth.[3]

Following Bilger,[13] the laminar flamelet approximation was used to relate scalar properties to the mixture fraction. State relationships for the concentrations of major gas species were obtained from the laminar flame measurements. The state relationship for soot volume fractions was found from laser extinction measurements in both laminar and turbulent flames, as described later. State relationships for temperature and density were computed, assuming that each flame lost 60 percent of its chemical energy release by radiation , and using measured concentrations of major gas species from the state relationships. Thermochemical properties for these calculations were obtained from Gordon and McBride.[18]

Radiation Properties

The equation of radiative transfer was solved to find spectral intensities for radiation paths corresponding to the measurements. This involved a Goody statistical narrow-band model with the Curtis-Godson approximation for inhomogeneous gas paths, following Ludwig et al.[19] The computer program RADCAL, developed by Grosshandler,[20] was used for the calculations, considering the gas bands of CO_2, CO, H_2O and CH_4 as well as continuum radiation from soot at the small-particle limit, e.g., scattering was ignored.

Turbulence/radiation interactions were either ignored, by basing predictions on mean properties, or considered, by using a stochastic method. The mean-property method employed time-averaged mean scalar properties, found from the structure computations, along the radiation path. The stochastic method involved dividing the radiation path into dissipation-scale sized eddies which were assumed to have uniform properties at each instant. The probability density function of mixture fraction for each eddy was randomly sampled to provide a realization of scalar properties along the path, in conjunction with the state relationships. Spectral radiation intensities were then computed for each realization, similar to the mean-property method. Sufficient realizations were averaged to obtain statistically-significant results.

Radiative heat fluxes were computed using the mean-property method, in conjunction with the discrete-transfer approach of Lockwood and Shah.[21] This involves summing spectral radiation intensities for various paths through the flame (120 to cover the field of view) and for the wavelength range having significant radiance (500 - 6000 nm), allowing for the cut-off of the sapphire window of the sensor.[15]

Results and Discussion

State Relationships

Concentrations of O_2, N_2, CO_2, CO, CH_4, C_2H_6, H_2O, H_2 and C_2H_2, measured in the laminar flames, are plotted as a function of fuel-equivalence ratio (which is a single-valued function of mixture fraction) in Figs. 1 and 2. Three different axial stations and two fuel flow rates were considered, however, only the latter are identified to reduce clutter of the figures. Fuel-equivalence ratios were calculated based on the total carbon in all gas species and nitrogen, neglecting ambient carbon monoxide and water vapor, and assuming that the local carbon-to-hydrogen ratio was the same as the fuel. To reduce uncertainties in this procedure, positions involving significant concentrations of soot are not considered.

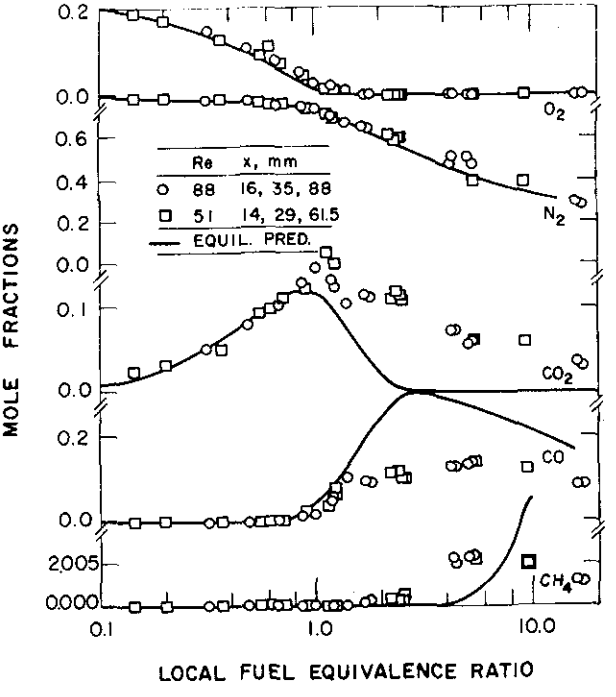

Fig. 1 State relationships for gas concentrations in acetylene/air diffusion flames.

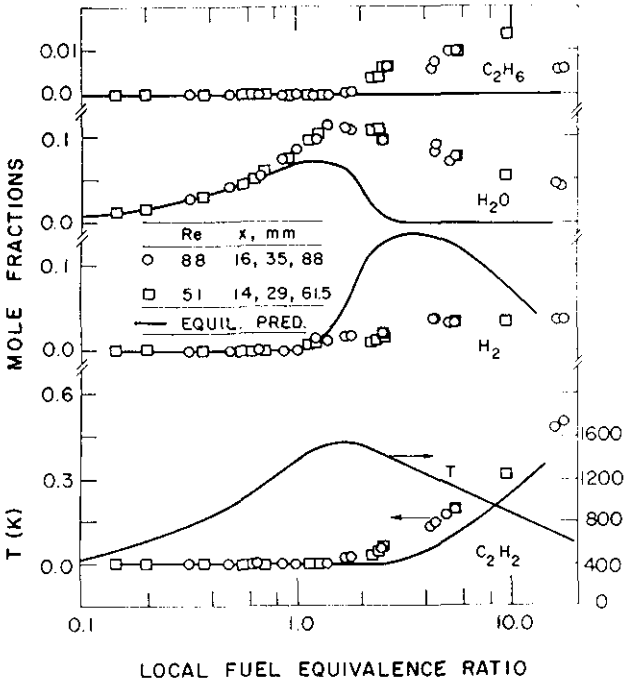

Fig. 2 State relationships for gas concentrations in acetylene/air diffusion flames (continued).

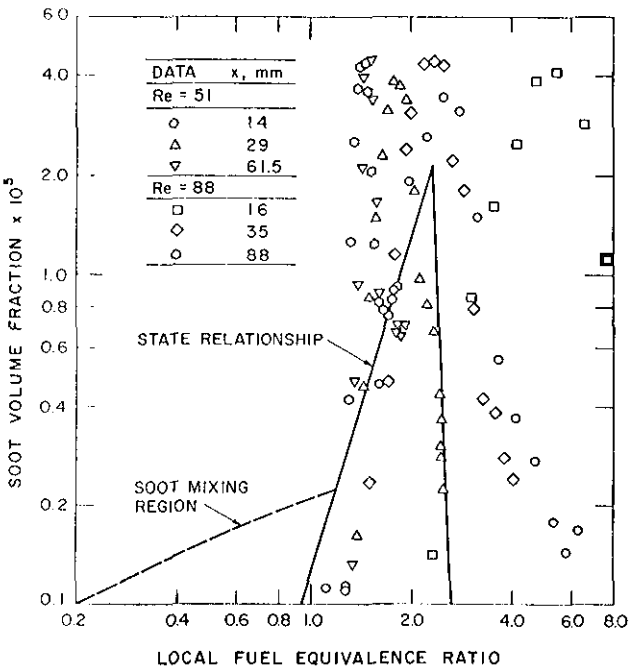

Fig. 3 State relationship for soot volume fraction in acetylene/air diffusion flames.

However, soot particles do not diffuse like gas molecules; therefore, local carbon/hydrogen ratios could differ from the original fuel, even though soot concentrations are small. Uncertainties due to this effect are difficult to quantify, however, they are unlikely to exceed uncertainties in the concentration measurements themselves. Predictions based on the Gordon and McBride code[19] (assuming thermodynamic equilibrium, no solid carbon present, and adiabatic combustion) also appear on the figures.

Measurements illustrated in Figs. 1 and 2 approximate local thermodynamic equilibrium for fuel-lean conditions, providing an immediate explanation for universal correlations of gas species concentrations in this region. Concentrations depart appreciably from equilibrium predictions for fuel-rich conditions; however, they still yield reasonably universal correlations as a function of fuel-equivalence ratio, satisfying the laminar flamelet approximation. Attainment of quasi-equilibrium for fuel-rich conditions is typical of other hydrocarbons that have been studied.[3,4,8,13,14] Whether this behavior persists in regions having high concentrations of soot is unknown, however, results discussed next show that this involves a relatively narrow range of mixture fractions in any event.

Measurements of soot volume fractions for the laminar flame are plotted as a function of fuel-equivalence ratio in Fig. 3. As just noted, the highest concentrations of soot are confined to a relatively narrow range of fuel-equivalence ratios, just on the rich side of the diffusion flames. Species concentrations could not be measured in this soot layer; therefore, fuel-equivalence ratios were estimated by interpolating plots of fuel-equivalence ratio as a function of distance for a given height above the burner, as described by Gore.[15] The uncertainty of this procedure is highest near the burner exit.

Results illustrated in Fig. 3 indicate that maximum soot volume fractions are relatively independent of burner flow rate and height above the burner. Only positions nearer the burner exit exhibit lower peak soot volume fractions which are indicative of effects of finite-rate chemistry.[15] Maximum soot volume fractions are roughly 8 times larger than in ethylene/air diffusion flames. Except for the lowest traverse at the highest Reynolds number (x/d = 16, Re = 88), the results are crudely universal in view of potential uncertainties in estimations of fuel-equivalence ratios. However, there is a progressive shift in the location of the maximum soot volume fraction toward lower fuel-equivalence ratios with increasing distance above the burner that was not seen in the ethylene/air diffusion flames.[8] This behavior is probably due to convection since soot particles do not diffuse like gas molecules. The flow properties of the present laminar flames cause soot particles to be convected toward the flame axis near its base and away from the flame axis near its tip. Convection of soot particles by this motion would cause soot concentrations to shift toward rich conditions near the base of the flame and lean conditions near the tip, as seen in Fig. 3. Naturally, such hydrodynamic effects preclude exact universality of soot volume fractions in laminar flames, and effects of hydrodynamics are likely to be different in turbulent flames as well. Nevertheless, the divergence from universality for the laminar measurements illustrated in Fig. 3 is not large in comparison to other uncertainties concerning soot concentrations in turbulent flames; therefore, use of a soot volume fraction state relationship was pursued.

The soot volume fraction state relationship illustrated in Fig. 3 was constructed using the laminar measurements as well as laser extinction measurements in the turbulent flames, similar to the approach used earlier for ethylene/air diffusion flames.[8] The laminar and turbulent flames both emitted soot; therefore, the state relationship was extended into the fuel-lean region (the soot mixing region portion of the curve) to fit measurements of laser extinction above the flame tip. This portion was found by selecting a soot volume fraction at a fuel-equivalence ratio of 1.25 and computing values at leaner conditions using mixing analysis neglecting any subsequent oxidation of soot. The maximum soot volume fraction and the width of the state relationship in the fuel-rich region were also somewhat optimized using the extinction measurements in the turbulent flames. The final result crudely resembles the laminar measurements in the fuel-rich region, but differs by allowing

for soot emission in the fuel-lean region which does not occur near the base of the present laminar flames.

Flame Structure

Structure results for the two turbulent flames were similar; therefore, only the findings for the higher Reynolds number flame will be considered. Predicted and measured mean and fluctuating streamwise velocities and mean gas species concentrations along the axis are illustrated in Fig. 4. Time-averaged velocities were measured while the analysis only provides Favre-averaged velocities. Differences between these averages are typically less than 10 percent for mean velocities along the axis of turbulent diffusion flames.[22] However, time-averaged velocity fluctuations can be up to 40 percent greater than Favre averages near the tip of turbulent diffusion flames (roughly x/d = 80 in the present case.)[22] Furthermore, the analysis only provides k; therefore, $\tilde{u}''$ has been estimated assuming isotropic turbulence ($\tilde{u}''^2 = 2k/3$). Usual levels of anisotropy along the axis of turbulent diffusion flames would yield values roughly 20 percent higher.[22] In view of these observations, the comparison between predicted and measured velocities is reasonably good. However, velocity fluctuations are still somewhat underestimated in the region beyond the flame tip (and to even a greater degree in the lower Reynolds number flame[15]). This behavior has been observed during all past evaluations of flame structure in this laboratory.[1-8] The effect is attributed to neglecting turbulence/buoyancy interactions in the governing equations for turbulence quantities during the present formulation.[1]

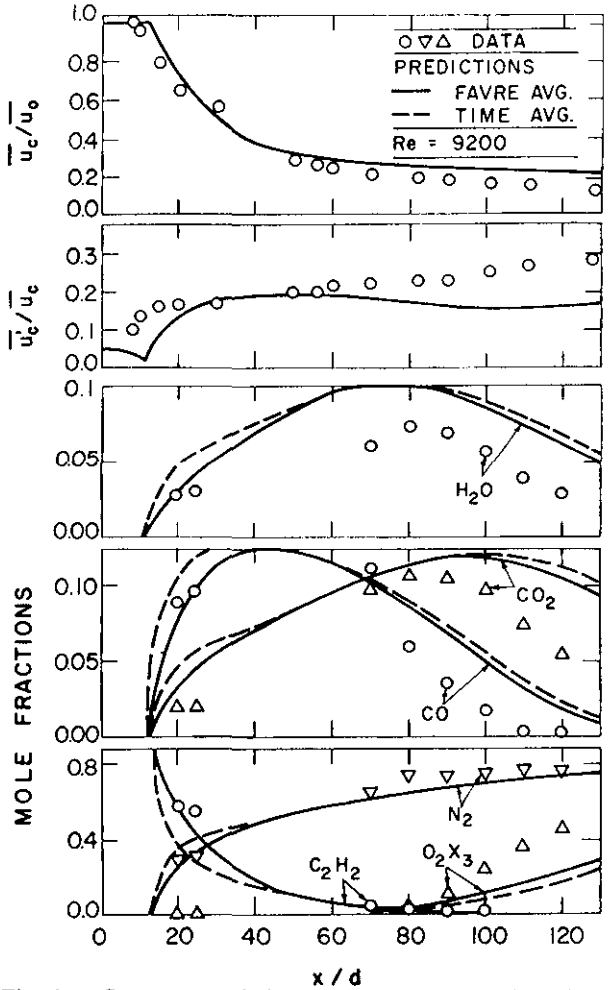

Fig. 4 Structure predictions and measurements along the axis of an acetylene/air diffusion flames. Re = 9200.

The analysis provides both Favre- and time-averaged predictions of scalar properties; therefore, both are plotted in Fig. 4. The degree of density weighting of the measurements is unknown;[22] however, differences between these averages are not large for the concentrations of major gas species. Samples could not be obtained in regions having high soot concentrations; this accounts for the gaps in the data illustrated in Fig. 4. There is fair agreement between predictions and measurements, sufficient to proceed to evaluation of radiation properties. However, predictions are generally poorer than in the past,[1-8] particularly near and beyond the flame tip where predictions clearly underestimate the rate of development of the flow.

Several reasons can be advanced for the poorer performance of the structure analysis for the present flames than in the past. First of all, the large radiative heat loss fraction implies significant energy exchange within the flame. This causes energy exchange between the reaction zone and soot in the lean portions of the flame, with resulting effects of buoyancy near the edge of the flow increasing rates of entrainment and mixing. This would cause more rapid development of the flow than present predictions where this effect is neglected. A second difficulty could be purely an experimental problem. The large concentration of soot emitted by these flames required larger blower exhaust rates than in the past, in order to prevent recirculation of soot into the test area. This tends to increase ambient disturbances in the upper portions of the flame, enhancing mixing rates. A final difficulty involves use of a lower initial turbulence kinetic energy for initial calculations illustrated here, than was actually measured (compare Fig. 4 and Table 1). This reduces predicted initial rates of development of the flow, contributing to underestimation of development rates far from the injector. This last difficulty is being rectified by computations that are currently in progress.

Spectral Absorption Properties

Soot properties of the turbulent flames were evaluated using light-sheet photographs as well as laser extinction predictions and measurements. The light-sheet photographs recorded Mie scattering from soot particles in the flames. They were obtained by sweeping the unfocussed beam of a 4W cw argon-ion laser (all-lines mode) in a vertical plane through the flame axis. Photographs were obtained with the camera shutter open for one sweep of the laser. Sweep speeds yielded illumination times on the order of 10 μs at each point in the flow, which effectively stopped the motion of the soot particles.

A typical light-sheet photograph appears in Fig. 5. The region seen is near the tip of the Re = 5300 flame, covering x/d = 80-90. This region was inside the luminous boundary of the flame at the instant that the photograph was obtained. The photograph shows that the soot is confined to streaks, probably associated with the eddy structure of the flame, similar to the earlier observations of Magnussen.[11] The results generally agree with the soot volume fraction state relationship illustrated in Fig. 3, with the finite-width streaks being associated with the narrow range of fuel-equivalence ratios where soot volume fractions are high enough to scatter appreciable amounts of light. Other photographs, having a larger field view and higher in the overfire region, show the streak pattern merging with broader regions of low-level scattering which is characteristic of the soot mixing region.[15]

Predictions and measurements of laser extinction by soot for the two turbulent flames appear in Figs. 6 and 7. Measurements for the two laser wavelengths (514 and 632.8 nm) are consistent with the reciprocal-wavelength dependence of extinction coefficients at the small-particle limit, justifying this approximation in the analysis.[15] Three sets of

Fig. 5 Light-sheet photograph of soot particles in an acetylene/air diffusion flame. Re = 5300.

predictions for extinction at 632.8 nm appear on the figures, as follows: (1) the mean-property method with the complete state relationship for soot, denoted MEAN,BT; (2) the stochastic method with the complete state relationship for soot, denoted STOCH,BT; and (3) the stochastic method but ignoring the mixing region of the soot state relationship, denoted STOCH,NBT.

Differences between the mean-property and stochastic predictions are not very significant in Figs. 6 and 7, indicating small effects of turbulence/radiation interactions for extinction. This finding is similar to earlier results for soot-containing ethylene/air diffusion flames.[8] The role of soot in the lean region can be seen by comparing results with and without the soot-mixing portion of the state relationships. Results for the upper positions show that neglecting the soot-mixing region causes substantial underestimation of extinction. In contrast, measurements at the lowest position are better represented by omitting the soot mixing region, although this might be fortuitous due to underestimation of flame widths.[15] It is also plausible, however, that the flames do not emit much soot near their base, similar to findings for the laminar flames.

The absolute agreement between predictions using the complete state relationships for soot and the measurements is reasonably good in Figs. 6 and 7, aside from some overestimation of extinction at the lowest position -- noted earlier. Results at the upper positions were fitted to some extent when the state relationship was constructed; therefore, good agreement is perhaps not very surprising. Nevertheless, it is encouraging that a single state relationship for soot volume fraction is able to treat effects of position and flow rate reasonably well, for present test conditions.

Radiation Emission Properties

Measurements and predictions of spectral radiation intensities are illustrated in Figs. 8 and 9. Results are presented for three axial stations, representing locations before, near, and after the flame tip (which is at x/d = 70 - 80 for these flames). Predictions are based on the complete state relationship for soot

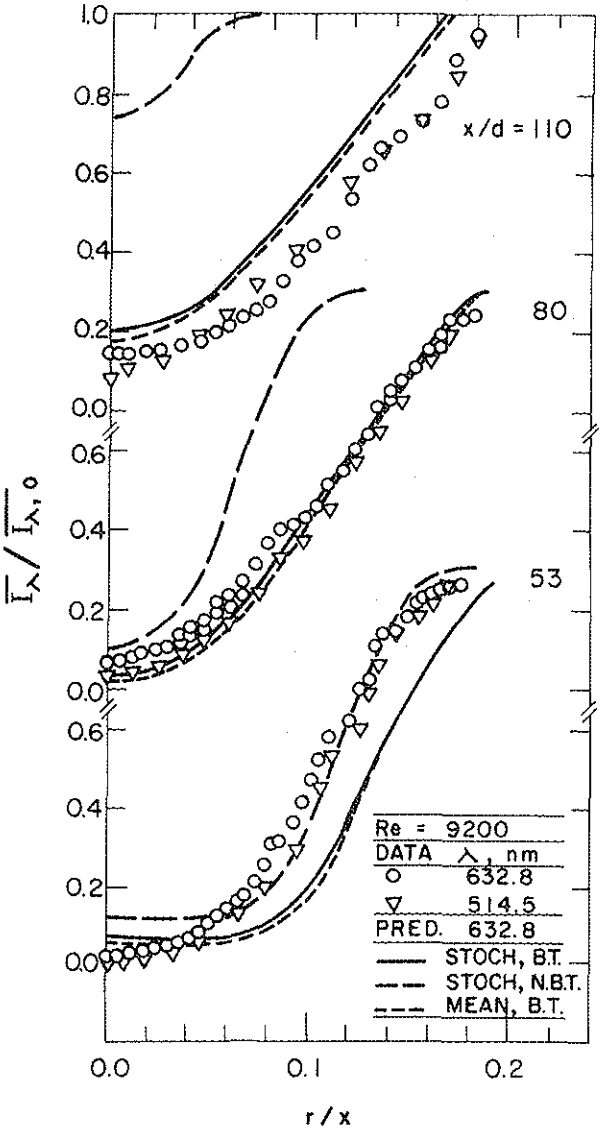

Fig. 6. Monochromatic transmittancies for an acetylene/air diffusion flame. Re = 9200.

volume fraction, both ignoring and considering effects of turbulence/radiation interactions.

The spectra in Figs. 8 and 9 are dominated by continuum radiation from soot, however, gas bands at 1140, 1870, 2700 and particularly 4300 nm can still be seen. Spectral intensities are highest at x/d = 53, which is somewhat before the tip of the turbulent flames. This differs from flames studied earlier where maximum spectral intensities have been generally associated with the flame tip.[1-8] One reason for this is that soot volume fractions, which strongly influence continuum radiation levels, peak at fuel-rich conditions -- shifting peak radiation levels accordingly. Another factor could be reduced emission of soot in the lower portions of the flame, which was suggested by the laser extinction measurements. If this occurs, higher intensities in this region result from reduced absorption by soot particles in the lean portions of the flame. A third effect involves energy losses by radiation from the flame, tending to reduce temperatures near the flame tip. This behavior would be most noticeable for the present acetylene/air diffusion flames, due to their high radiative heat loss fractions, in comparison to flames considered earlier.[1-8]

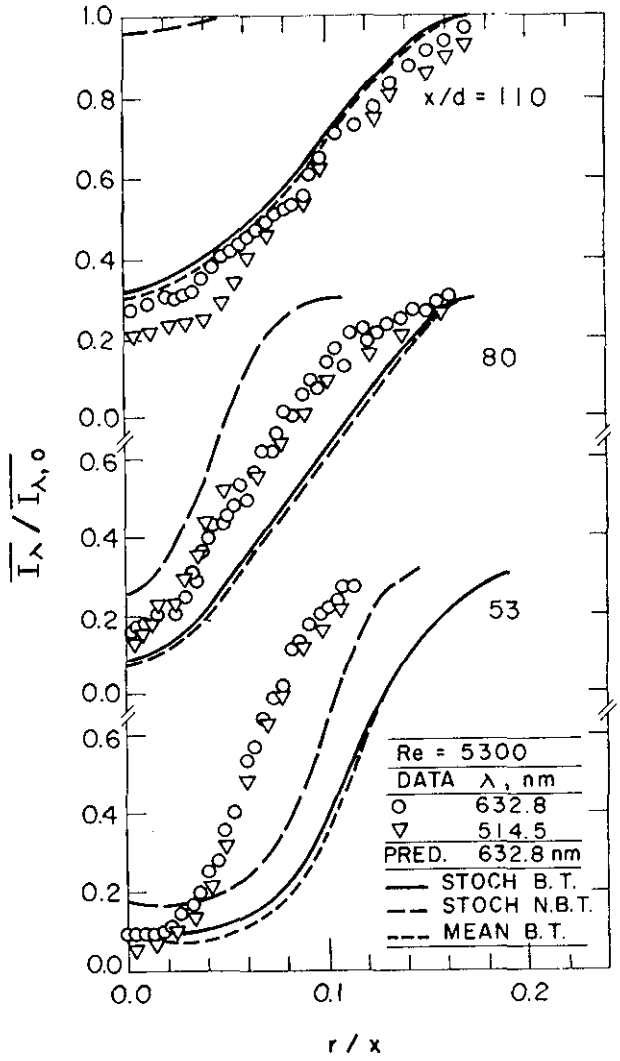

Fig. 7. Monochromatic transmittancies for an acetylene/air diffusion flame. Re = 5300.

Differences between mean property and stochastic predictions illustrated in Figs. 8 and 9 suggest significant turbulence/radiation interactions (50 - 300 percent) for continuum radiation emission from the turbulent flames. Since extinction results were affected very little by turbulence/radiation interactions, the nonlinearity of the Plank function with temperature is probably the main cause of this behavior. This suggests similar effects for other luminous flames having appreciable continuum radiation.

Predictions and measurements are qualitatively similar in Figs. 8 and 9, however, quantitative agreement is poorer for the present flames than for ethylene/air diffusion flames,[8] and certainly for the nonluminous flames.[1-7] Several reasons can be advanced for this behavior. First of all, the structure analysis tends to underestimate the rate of development of the flames, particularly beyond the flame tip, as noted earlier. This causes spectral intensities to be underestimated at x/d = 110, since spectral intensities decrease rapidly with streamwise distance in this region. Next, emission is also a sensitive function of local temperatures; therefore, neglecting internal energy exchange by radiation could be a factor in the increased discrepancies between predictions and measurements, particularly since radiation exchange is so large for the present flames. Finally, reduced emission of soot in the lower regions of the flames would also contribute to errors when a single state

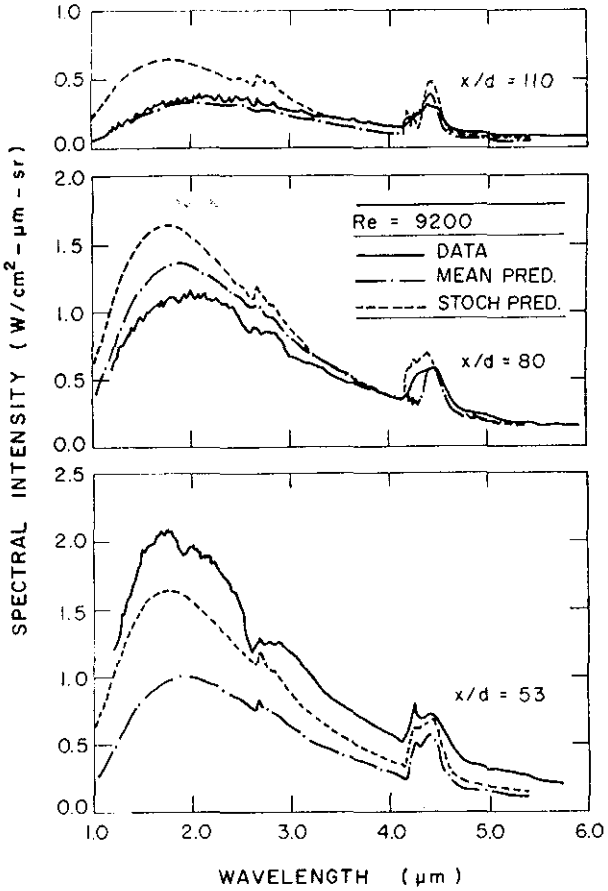

Fig. 8. Spectral radiation intensities for an acetylene/air diffusion flame. Re = 9200.

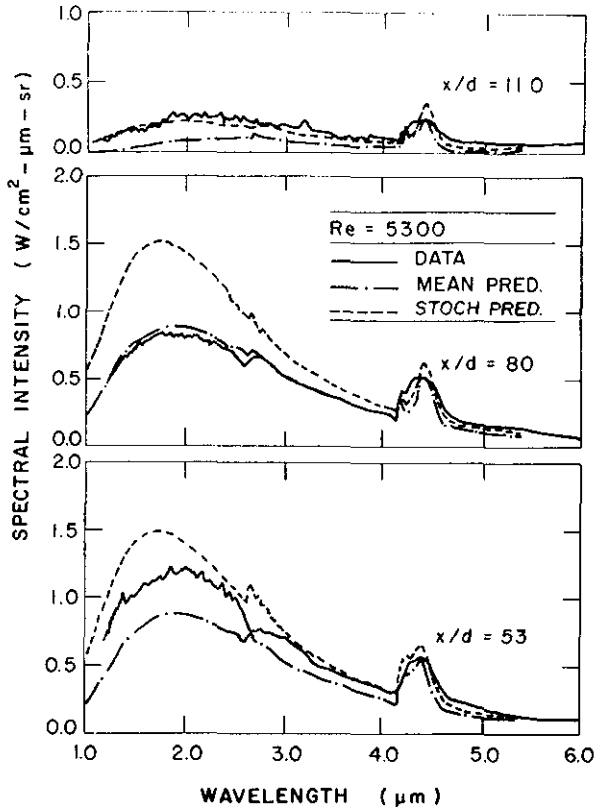

Fig. 9. Spectral radiation intensities for an acetylene/air diffusion flame. Re = 5300.

relationship is used for the predictions. This would help explain why the predictions underestimate spectral intensities at Re = 9200 and x/d = 53.

Measurements and predictions of radiative heat flux distributions around the two turbulent flames are illustrated in Figs. 10 and 11. Predictions are based on the mean-property method. Figure 10 is an illustration of radiative heat fluxes for a transducer facing the flame axis and traversed vertically at a distance of 575 mm from the axis. The radiative heat fluxes reach a maximum for the flames at x = 300 - 350 mm (x/d = 60 - 70) which is slightly on the fuel-rich side of the flame tips (x/d = 70 - 80). The predictions generally underestimate the measurements, consistent with the performance of the mean-property method for spectral intensities. The predictions generally treat effects of position and flow rate reasonably well, which is encouraging. However, effects of turbulence/radiation interactions and internal energy exchange within the flames, which were ignored during the present analysis, are very significant for these flames -- precluding close quantitative agreement between predictions and measurements.

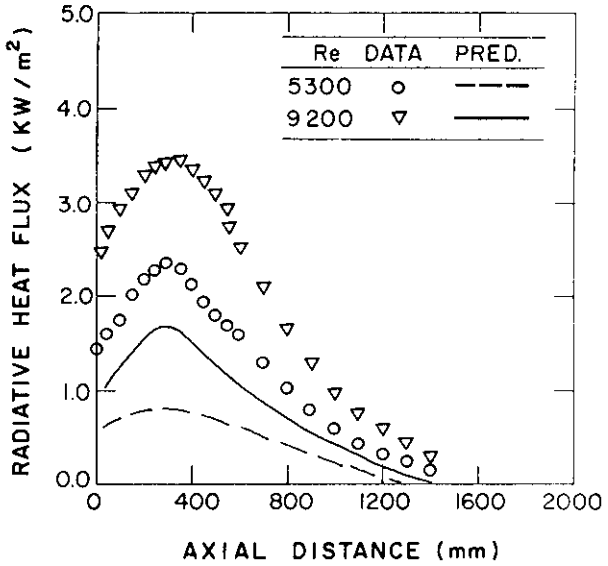

Fig. 10. Total radiative heat fluxes parallel to the axis of acetylene/air diffusion flames.

Measured and predicted radiative heat fluxes for a transducer facing vertically upward, and traversing in the radial direction in the plane of the base of the flames, are illustrated in Fig. 11. In this case, the heat flux is a maximum near the injector and decreases monotonically with increasing radial distance. The comparison between predictions and measurements is similar to Fig. 10.

Conclusions

Major conclusions of the study are as follows:

1. Study of both laminar and turbulent acetylene/air diffusion flames suggests nearly universal state relationships for the concentrations of major gas species.

2. Soot volume fractions in the laminar flames were much less universal than gas concentrations. Nevertheless, universality of soot volume fractions in turbulent flames appears to be a useful concept, which circumvents the complexities of soot chemistry in turbulent environments. The concept should be investigated further.

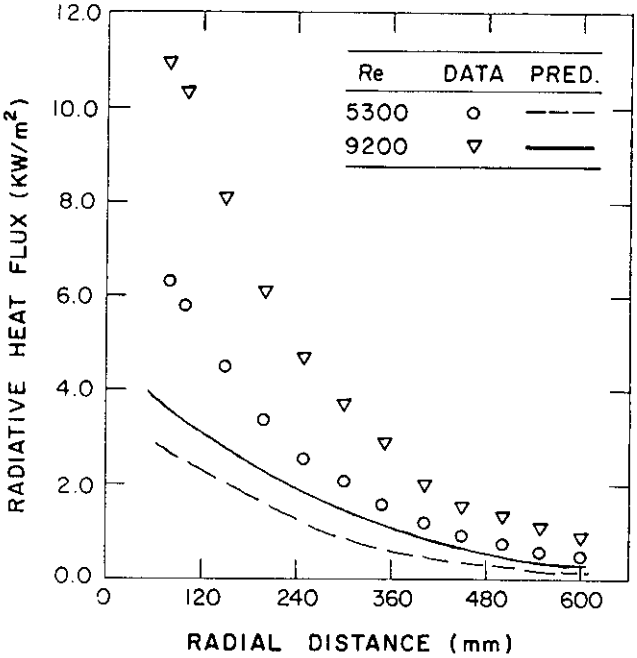

Fig. 11. Total radiative heat fluxes in the plane of the injector of acetylene/air diffusion flames.

3. Effects of turbulence/radiation interactions were significant for continuum radiation emission from soot (50 - 300 percent) but are not very important for absorption in the visible (514 and 632.8 nm). This suggests that turbulence/radiation interactions largely result from the strongly nonlinear dependence of the Plank function on temperature.

4. Structure and radiation emission predictions were less satisfactory for the present acetylene/air diffusion flames than for earlier work with luminous ethylene air flames.[8] The main reason for this behavior is the much larger radiative heat loss fraction, approaching 60 percent of the chemical energy release, for the present flames. This implies significant radiative energy exchange within the flames; therefore, coupled structure and radiation analysis should be considered in an effort to reduce present deficiencies in predictions.

Acknowledgements

This research was supported by the Center for Fire Research of the National Bureau of Standards, Grant No. 60NANB5D0576, with Dr. B.J. McCaffrey serving as NBS Scientific Officer. The authors also wish to acknowledge the assistance of D. Hully during measurements of state relationships.

References

1 Jeng, S.-M., Chen, L.-D. and Faeth, G.M., "The Structure of Buoyant Methane and Propane Diffusion Flames," Nineteenth Symposium (International) on Combustion, The Combustion Institute, Pittsburgh, 1982, pp. 349-358.

2 Jeng, S.-M., Lai, M.-C. and Faeth, G.M., "Nonluminous Radiation in Turbulent Buoyant Axisymmetric Flames," Comb. Sci. and Tech., Vol. 40, Sept. 1984, pp. 41-53.

3 Jeng, S.-M. and Faeth, G.M., "Species Concentrations and Turbulence Properties in Buoyant Methane

Diffusion Flames," J. Heat Trans., Vol. 106, Nov. 1984, pp. 721-727.

4 Jeng, S.-M. and Faeth, G.M., "Predictions of Mean Scalar Properties in Turbulent Propane Diffusion Flames," J. Heat Trans., Vol. 106, Nov. 1984, pp. 891-893.

5 Jeng, S.-M. and Faeth, G.M., "Radiative Heat Fluxes Near Turbulent Buoyant Methane Diffusion Flames," J. Heat Trans., Vol. 106, Nov. 1984, pp. 886-888.

6 Gore, J.P., Jeng, S.-M. and Faeth, G.M., "Spectral and Total Radiation Properties of Turbulent Carbon Monoxide/Air Diffusion Flames," AIAA J., in press.

7 Gore, J.P., Jeng, S.-M. and Faeth, G.M., "Spectral and Total Radiation Properties of Turbulent Hydrogen/Air Diffusion Flames," J. Heat Trans., in press.

8 Gore, J.P. and Faeth, G.M., "Structure and Spectral Radiation Properties of Turbulent Ethylene/Air Diffusion Flames," Twenty-First Symposium (International) on Combustion, The Combustion Institute, Pittsburgh, in press.

9 Dalzell, W.H. and Sarofim, A.F., "Optical Constants of Soot and their Application to Heat-Flux Calculations," J. Heat Trans., Vol. 91, pp. 100-104, 1969.

10 Beier, R.A., Pagni, P.J. and Okoh, C.I., "Soot and Radiation in Combustion Boundary Layers," Comb. Sci. and Tech., Vol. 39, 1984, pp. 235-262.

11 Magnussen, B.F., "An Investigation into the Behavior of Soot in a Turbulent Free Jet C_2H_2-Flame," Fifteenth Symposium (International) on Combustion, The Combustion Institute, Pittsburgh, 1974, pp. 1415-1425.

12 Kent, J.H. and Bastin, S.J., "Parametric Effects on Sooting in Turbulent Acetylene Diffusion Flames," Comb. Flame, Vol. 56, 1984, pp. 29-42.

13 Bilger, R.W., "Reaction Rates in Diffusion Flames," Comb. Flame, Vol. 30, 1977, pp. 277-284.

14 Liew, S.K., Bray, K.N.C. and Moss, J.B., "A Flamelet Model of Turbulent Non-Premixed Combustion," Comb. Sci. and Tech., Vol. 27, 1981, pp. 69-73.

15 Gore, J.P., "A Theoretical and Experimental Study of Turbulent Flame Radiation," Ph.D. Thesis, The Pennsylvania State University, University Park, PA, 1986.

16 Santoro, R.J., Semerjian, H.B. and Dobbins, R.A., "Soot Particle Measurements in Diffusion Flames," Comb. Flame, Vol. 51, 1983, pp. 203-218.

17 Bilger, R.W., "Turbulent Jet Diffusion Flames," Prog. Energy Combust. Sci., Vol. 1, 1976, pp. 87-109.

18 Gordon, S. and McBride, B.J., "Computer Program for Calculation of Complex Chemical Equilibrium Compositions, Rocket Performance, Incident and Reflected Shocks, and Chapman-Jouget Detonations," NASA SP-273, 1971.

19 Ludwig, C.B., Malkmus, W., Reardon, J.E. and Thomson, J.A., Handbook of Infrared Radiation from Combustion Gases, NASA SP-3080, 1973.

20 Grosshandler, W.L., "Radiative Heat Transfer in Nonhomogeneous Gases: A Simplified Approach," Int. J. Heat Mass Trans., Vol. 23, 1980, pp. 1447-1459.

21 Lockwood, F.C. and Shah, N.B., "A New Radiation Solution Method for Incorporation in General Combustion Prediction Procedures," Eighteenth Symposium (International) on Combustion, The Combustion Institute, Pittsburgh, 1981, pp. 1405-1414.

22 Faeth, G.M. and Samuelsen, G.S., "Fast-Reaction Nonpremixed Combustion," Prog. Energy Combust. Sci., in press.